

Imaging of facial nerve schwannomas: diagnostic pearls and potential pitfalls

Pravin Mundada
Bela Satish Purohit
Tahira Sultana Kumar
Tiong Yong Tan

ABSTRACT

Schwannomas are uncommon in the facial nerve and account for less than 1% of tumors of temporal bone. They can involve one or more than one segment of the facial nerve. The clinical presentations and the imaging appearances of facial nerve schwannomas are influenced by the topographical anatomy of the facial nerve and vary according to the segment(s) they involve. This pictorial essay illustrates the imaging features of facial nerve schwannomas according to their various anatomical locations and also reviews the pertinent differential diagnoses and potential diagnostic pitfalls.

Facial nerve schwannomas (FNSs) are rare slow-growing tumors, accounting for less than 1% of all temporal bone tumors. They are typically solitary, unilateral, and sporadic in nature. FNSs may be bilateral as part of neurofibromatosis-2 spectrum (1, 2). Rarely, multiple schwannomas may involve peripheral branches of the facial nerve (FN) (3). The age of presentation varies from 5 to 84 years. No gender or side predilection is seen (4, 5).

Histologically, FNSs are neuroectodermal in origin. They are encapsulated, benign tumors arising from the Schwann cells. They may show intratumoral cystic change and hemorrhage (3, 4, 5). Malignant schwannoma of the FN is extremely rare (6). FNSs commonly present with peripheral facial neuropathy and/or various otologic symptoms including sensorineural and conducting hearing loss (2–5). Facial paralysis is often seen at a later stage or may not be seen at all. The reasons for this are thought to be neuronal tolerance induced by the extremely slow growth of the tumor, abundant tumor vascularity, and commonly associated dehiscence of adjacent bone (7). Occasionally, FNSs may present as an intraparotid mass or as an intracranial lesion (2–5).

The clinical presentations and the imaging appearances of FNSs are influenced by the topographical imaging anatomy of the FN and vary according to the segment(s) they involve (8). Here, we briefly describe the anatomy of the FN, followed by general imaging features of FNSs on computed tomography (CT) and magnetic resonance imaging (MRI), and appropriate imaging protocols. Tumor involving each segment is reviewed in relation to its characteristic clinical presentations emphasizing diagnostic pearls and potential pitfalls. The imaging examples of FNSs illustrated in this pictorial review are all histopathologically proven cases.

Segmental anatomy of the facial nerve

The course of the FN is divided into six segments and two genua which are as follows: 1) cerebellopontine cistern (CPC) segment; 2) internal acoustic canal (IAC) segment; 3) labyrinthine segment; 4) geniculate ganglion (GG)/anterior genu; 5) tympanic segment; 6) posterior genu; 7) intramastoid segment; 8) extracranial segment. Each segment of the FN is closely related to several important structures, which may get affected by the expansion of the FN canal caused by the FNS (Figs. 1–5). The FN gives several branches along its course which are as follows: the greater superficial petrosal nerve (GSPN), muscular branches to the stapedius, posterior belly of digastric and stylohyoid, the chorda tympani, the posterior auricular nerve, and five terminal branches (temporal, zygomatic, buccal, marginal mandibular, and cervical) (9, 10).

From the Department of Radiology (P.M. ✉ mundada.pravin@gmail.com, T.S.K., T.Y.T.), Changi General Hospital, Singapore; Department of Radiology (B.S.P.), National Neuroscience Institute, Singapore.

Received 14 March 2015; revision requested 22 April 2015; revision received 20 May 2015; accepted 16 June 2015.

Published online 2 November 2015.
DOI 10.5152/dir.2015.15060

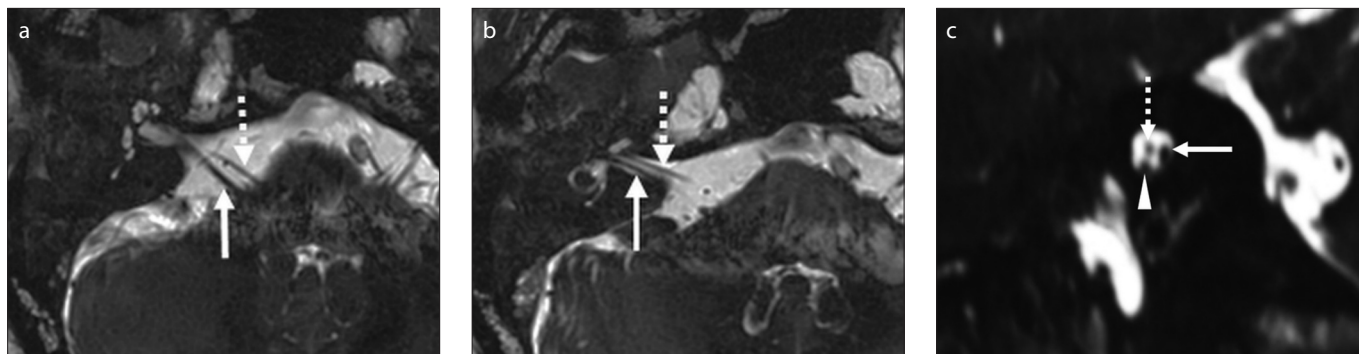


Figure 1. a–c. Anatomy of the right facial nerve (FN) on axial (a, b) and sagittal (c) high-resolution heavily T2-weighted images. The cerebellopontine cistern (CPC) segment of FN (a, dotted arrow) is related to the vestibulocochlear nerve posteriorly (a, arrow). The internal acoustic canal (IAC) segment of FN (b and c, dotted arrow) is related to the cochlear nerve inferiorly (c, arrowhead) and the superior vestibular nerve posteriorly (b and c, arrow).

Imaging protocols and general imaging features of facial nerve schwannomas

The commonly performed imaging protocol for the evaluation of FNS includes high-resolution CT (HRCT) scan of the temporal bone with multiplanar reconstructions and pre- and postcontrast multiplanar MRI sequences centered on the IAC (axial 2 mm T1-weighted imaging, three-dimensional 0.6 mm heavily weighted T2-weighted imaging (CISS), axial 2 mm T2-weighted fat-saturated imaging, coronal 2 mm postcontrast T1-weighted fat-saturated imaging, and postcontrast isovoxel VIBE). A simultaneous MRI of the brain (5 mm

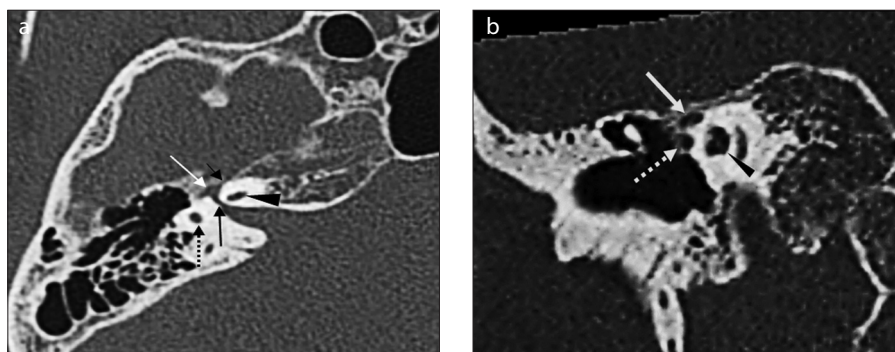


Figure 2. a, b. Anatomy of the right FN on axial (a) and coronal (b) HRCT images. The labyrinthine segment of FN (a, black arrow) is related to the cochlea anteromedially and slightly inferiorly (a, arrowhead) and to the semicircular canal posterolaterally (a, dotted black arrow), and ends at the geniculate ganglion (GG) (a, white arrow). The greater superficial petrosal nerve (GSPN) exits through the facial hiatus (a, short black arrow). The GG/anterior genu (b, white arrow) is related to tensor tympani inferiorly (b, dotted arrow) and cochlea posteromedially (b, arrowhead). It has a bony roof, which can be deficient in up to 18% of cases.

Main points

- Knowledge of the complex anatomical landscape of the facial nerve (FN) is vital in the diagnosis of facial nerve schwannomas (FNSs).
- The FNS involving the cisternal and/or internal acoustic canal segments of the FN cannot be confidently differentiated from the vestibular schwannoma on imaging. Its inclusion in the differential diagnosis of the latter has important implication in presurgical counselling.
- FNSs may present as a middle cranial fossa mass, a middle ear mass, an external auditory canal mass, or an intraparotid mass.
- Demonstration of smooth scalloping of the FN canal and adjacent bony labyrinth on HRCT differentiates the FNS from the FN hemangioma. However, FNSs of mastoid segment can sometimes mimic aggressive tumors.
- The differential diagnosis of an intraparotid mass with extension in the stylomastoid foramen includes FNS, parotid malignancy with perineural spread and, rarely, pleomorphic adenoma.

axial T2-weighted and 5 mm postcontrast T1-weighted sequences) is also routinely performed. Contrast-enhanced CT has no role in the imaging of FNS (2, 4).

FNSs usually involve more than one segment of the FN. Like schwannomas occurring elsewhere, FNSs are typically fusiform solid tumors with well-circumscribed smooth margins. They usually grow along the path of least resistance. They appear iso- to hypointense to brain parenchyma on T1-weighted images and hyperintense on T2-weighted images. On diffusion-weighted imaging, there is usually no restriction. They generally show homogeneous postcontrast enhancement; however, cystic degeneration may result in heterogeneous enhancement (2, 4). FNSs can show a “target sign” on T2-weighted images; however, this feature is nonspecific, and may be seen in other benign and malignant neurogenic tumors (3). Small FNSs cause smooth, fusiform expansion of the FN canal, best seen on HRCT images.

Large FNSs can cause pressure erosion of the adjacent bony labyrinth and ossicles. Bony erosions caused by FNSs are smooth and sharply margined, in keeping with long-standing bony compression rather than aggressive pathology (4, 5, 7).

Pearls and pitfalls in imaging of schwannomas according to involved facial nerve segment(s)

Schwannomas involving the CPC segment and/or the IAC segment of the FN cannot be differentiated from a vestibular schwannoma unless the tumor extends to the labyrinthine segment of the FN (Fig. 6). Other signs like erosion of superior part of the internal auditory canal and eccentricity of tumor in relation to porus acousticus are not reliable. Hence, it is imperative to include the FNS in the differential diagnosis of vestibular schwan-

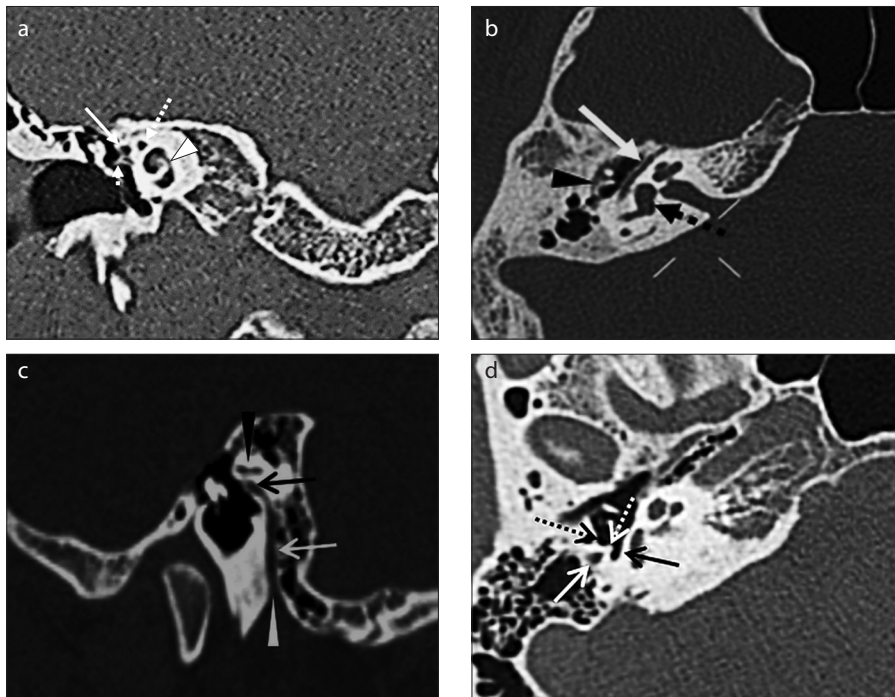


Figure 3. a–d. Anatomy of the right FN on axial (b, d), coronal (a), and sagittal (c) HRCT. The tympanic segment of FN (a and b, white arrow) is related to the lateral semicircular canal superiorly, labyrinthine segment of FN and cochlea medially (a, dotted white arrow and white arrowhead, respectively), the cochleariform process (a, short arrow) and the oval window inferiorly, the vestibule medially (b, black dotted arrow), and the incus laterally (b, black arrowhead). The posterior genu (c, black arrow) is related to the lateral semicircular canal superiorly (c, black arrowhead), fossa incudis superolaterally and the ponticulus superomedially. The intramastoid segment of FN (c and d, white arrow) is related to the facial recess anterolaterally (d, black dotted arrow), the pyramidal eminence anteriorly and the sinus tympani anteromedially (d, dotted white arrow and black arrow, respectively).

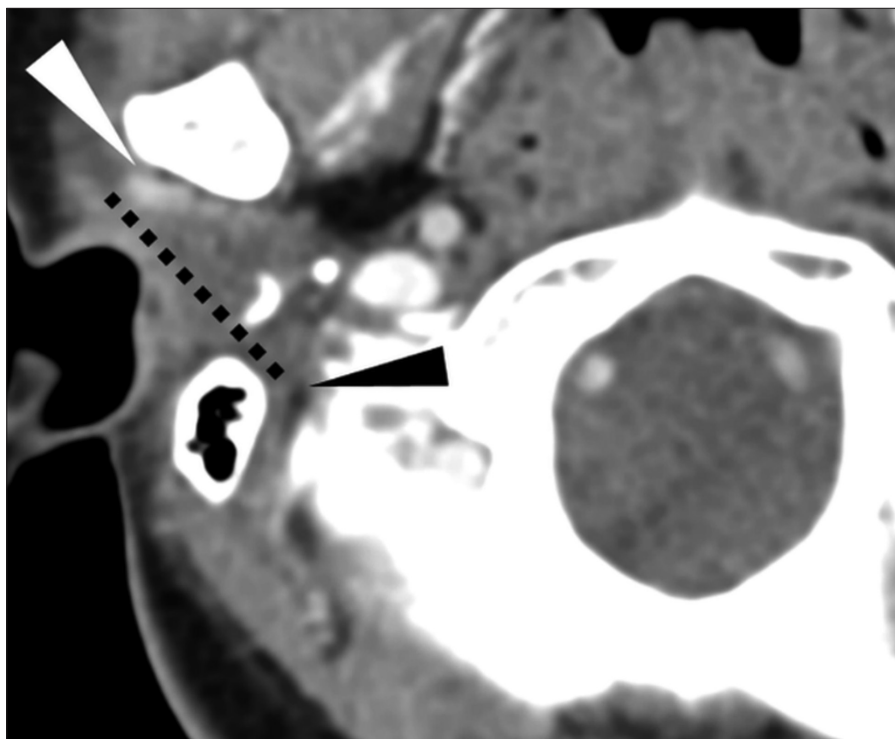


Figure 4. Anatomy of the right FN on axial postcontrast CT. The extra cranial segment of FN cannot be visualized on CT or MRI. Its course is marked by a line drawn from the stylomastoid foramen (black arrowhead) to the lateral aspect of the retromandibular vein (white arrowhead) where it enters in the parotid gland (dotted line).

noma during preoperative planning and counseling (2, 4, 5).

FNS may acquire a “dumbbell” shape when it shows multisegmental involvement. The relatively narrow labyrinthine segment forms the isthmus of the dumbbell between the globular tumor components at the IAC and the GG (Fig. 7). Occasionally, the GG component of a dumbbell-shaped FNS erodes into the cochlea and thus mimics a transmodiolar acoustic schwannoma. However, unlike FNS, a transmodiolar schwannoma expands the cochlear nerve canal but not the FN canal (11).

The GG fossa is the most common location for the occurrence of FNS. FNSs in this location often show extension to the tympanic and/or the labyrinthine segments. Isolated involvement of the GG at the time of presentation is very rare (Fig. 8). This location is also common for the occurrence of FN hemangiomas. In about 50% cases, FN hemangiomas may not show their characteristic amorphous honeycomb appearance and/or internal bony spicules on CT. However, FN hemangiomas show poorly defined margins on HRCT, which differentiate them from FNSs with smooth margins (12, 13).

A large FNS at the GG can cause bulbous expansion of the GG fossa, erosion of its roof, and can eventually present as an extra-axial middle cranial fossa mass (Fig. 9). Alternatively, it may extend anteriorly along the course of GSPN through the widened facial hiatus (Fig. 10). Rarely, it may involve the GSPN alone. Involvement of the GSPN by the tumor may be seen as smooth scalloping along the anterolateral margin of the petrous bone on CT (Fig. 10b). Whenever a middle cranial fossa mass is associated with facial nerve dysfunction and/or otologic symptoms, an FNS should be suspected (4, 12).

FNS of tympanic segment sometimes extends to the middle ear cavity by eroding the lateral wall of the FN canal. It can appear as a white mass behind an intact tympanic membrane on otoscopy. It can cause smooth pressure erosion of the tympanic cavity walls and of the ossicles. The ossicular chain may be disrupted (Fig. 11). FNS of tympanic segment can extend superomedially to cause smooth pressure erosion of the lateral semicircular canal and vestibule. Congenital cholesteatoma and middle ear adenoma may mimic FNS on otoscopy and CT, but the former shows no postcontrast enhancement and the latter shows no extension into the FN canal. Glomus tympanicum appears red on otoscopy and does not extend into the FN canal (4, 8, 12).

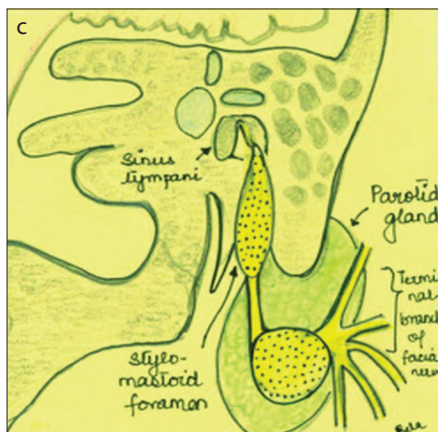
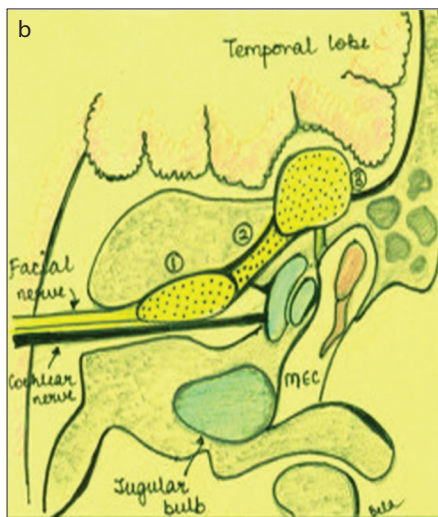
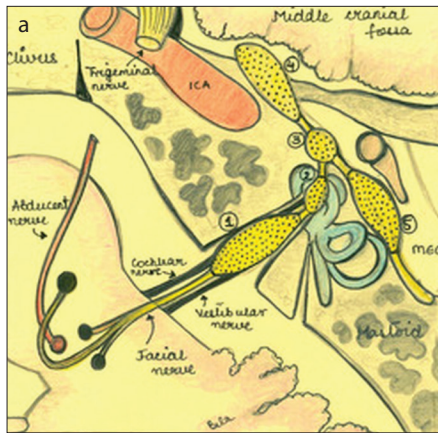


Figure 5. a–c. Schematic representation of axial section through IAC (a) shows anatomical context of facial nerve schwannoma (FNS), involving the IAC segment, the labyrinthine segment, the GG, the GSPN, and the tympanic segment of the left FN (a, 1 to 5, respectively). Schematic representation of the coronal section (b) through left IAC shows anatomical context of the FNS involving the IAC segment, the labyrinthine segment and the GG of the left FN and its extension to middle cranial fossa through the roof of the GG (b, 1 to 3, respectively). Schematic representation of the coronal section through the mastoid (c) shows anatomical context of FNS involving the mastoid and the intraparotid segments of the left FN.

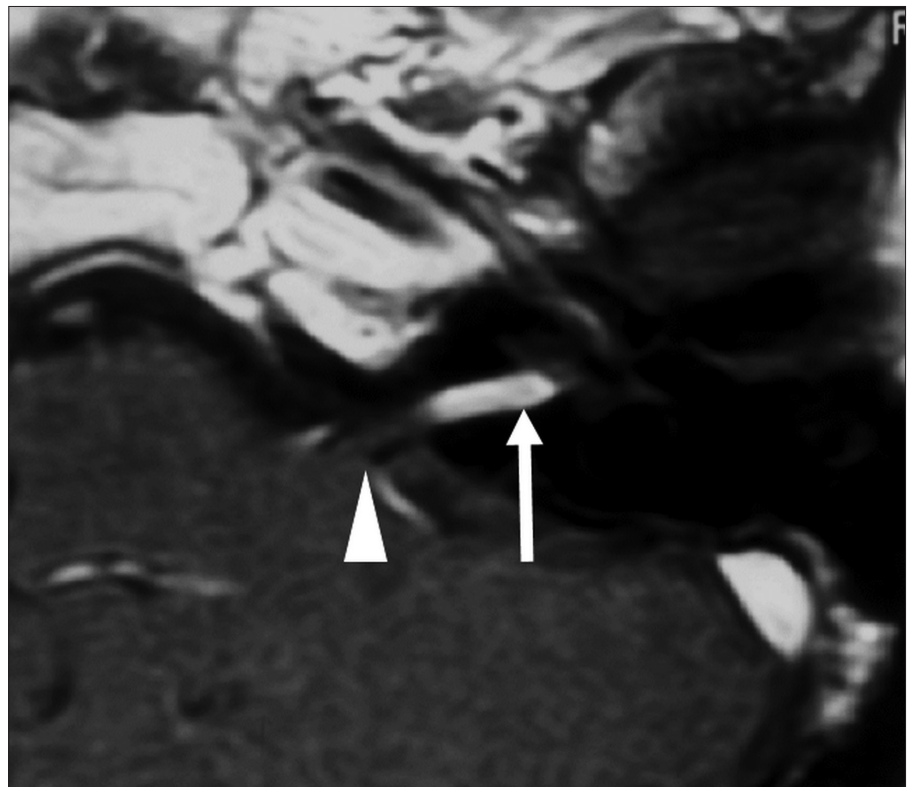


Figure 6. Contrast-enhanced axial T1-weighted image at the level of left IAC shows an intracanalicular enhancing mass (arrow). The CPC segment (arrowhead) and the labyrinthine segment (not shown) of the FN appear uninvolved. This mass, although proven to be an FNS on surgery, cannot be differentiated from a vestibular schwannoma on imaging.

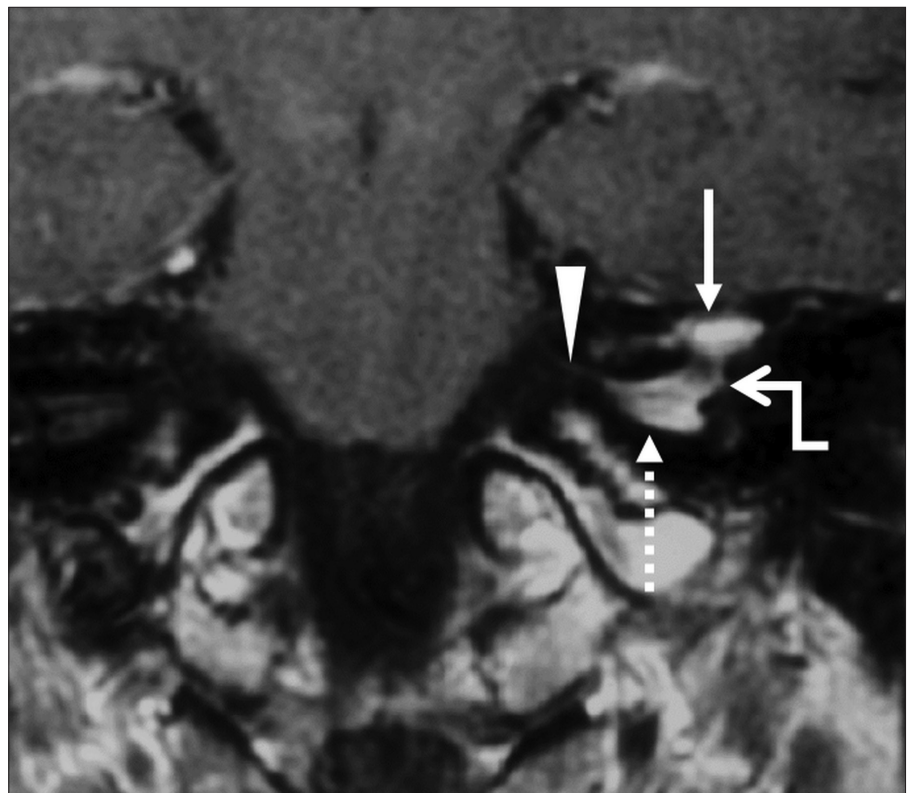


Figure 7. Contrast-enhanced coronal T1-weighted image through pons, at the level of the left IAC shows a dumbbell-shaped FNS. The isthmus of dumbbell is formed by the narrow labyrinthine segment of the FN (bent arrow), which connects the globular components in the IAC (dotted arrow) and those at the GG (arrow). The CPC segment of the FN (arrowhead) is not involved.

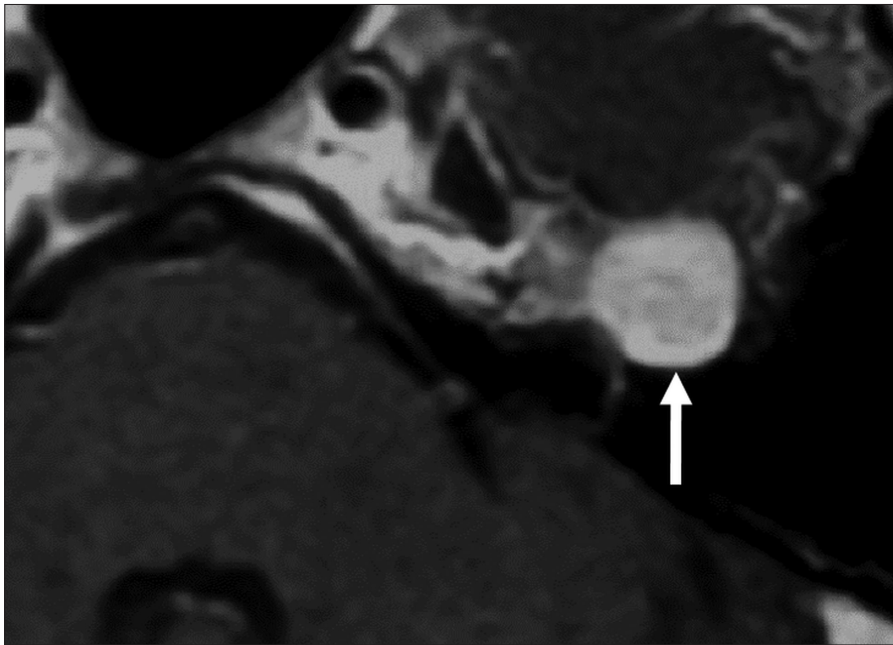


Figure 8. Contrast-enhanced axial T1-weighted image through the pons at the level of left internal auditory canal shows FNS involving the GG with no extension to other segments. This mass shows smooth scalloping of the adjacent bone on CT (not shown), which is compatible with FNS and excludes the possibility of a facial nerve hemangioma.

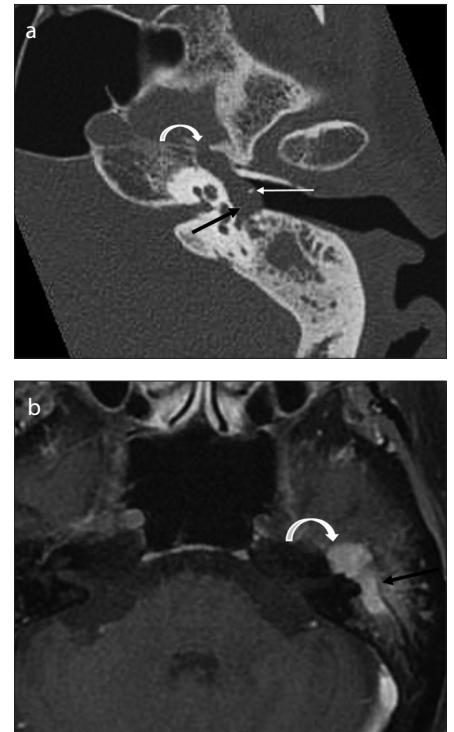


Figure 11. a, b. Axial HRCT (a) and postcontrast axial T1-weighted images (b) of left temporal bone through the IAC show fusiform-shaped FNS causing smooth erosion of the tympanic segment of FN, extending in the middle ear cavity (a and b, black arrow) and displacing the ossicle laterally (a, thin white arrow). It also causes smooth expansion of GG and the facial hiatus (a and b, white curved arrow).

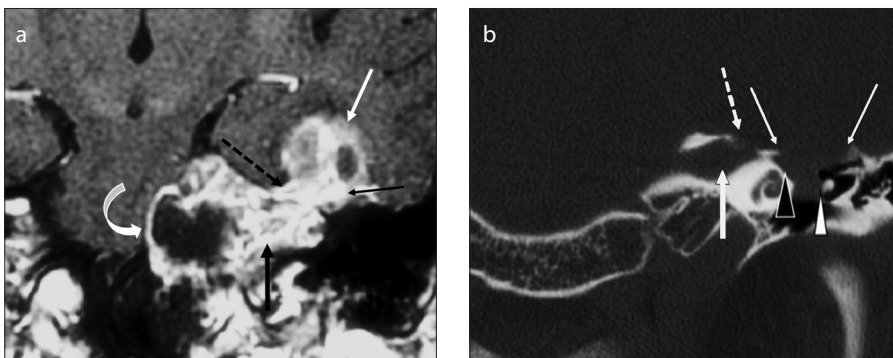


Figure 9. a, b. Contrast-enhanced coronal T1-weighted image (a) and coronal HRCT image (b) show a dumbbell-shaped FNS on left side. The FNS is involving the CPC segment (a, curved white arrow), IAC segment (a and b, thick black arrow), labyrinthine segment (a and b, dotted arrow), and the GG (a, thin black arrow). It is extending to the middle cranial fossa (a, white arrow) by eroding the roof of geniculate fossa (b, white arrows). The HRCT coronal image (b) shows smooth expansion of the facial nerve canal, and smooth erosion of the otic capsule (b, black arrowhead) and ossicles (b, white arrowhead).

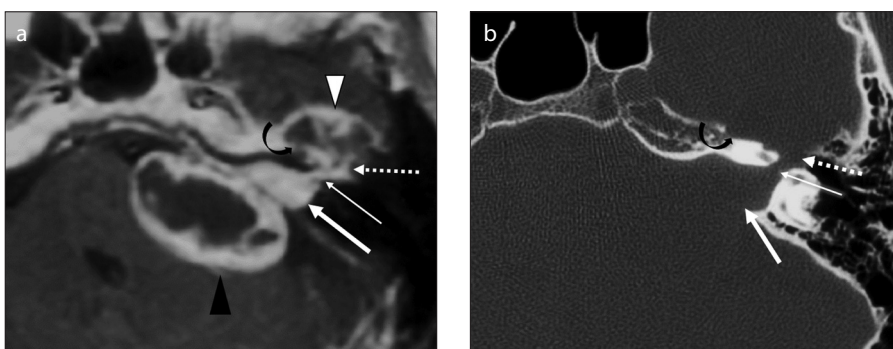


Figure 10. a, b. Contrast-enhanced axial T1-weighted image (a) and axial HRCT image (b) show a dumbbell-shaped FNS on the left side. The FNS is involving the CPC segment (a, black arrowhead), IAC segment (a and b, thick white arrow), labyrinthine segment (a and b, thin white arrow), and the GG (a and b, dotted white arrow). It is extending to the middle cranial fossa (a, white arrowhead) through the widened facial hiatus. Note its extension along the course of GSPN (a and b, curved black arrow). On HRCT axial image (b), the margins of the expanded FN canal appear smooth and well-defined without cortical destruction.

FNS involving the mastoid segment can cause smooth expansion of the vertical FN canal and can erode into the external auditory canal (Fig. 12). Occasionally, FNS of the mastoid segment may mimic aggressive bony lesions (like lymphoma or metastasis) when it breaks through the thin-walled adjacent mastoid air cells or shows irregular shape and margins on HRCT and postcontrast MRI (Fig. 13). Perineural spread of parotid gland malignancy along the FN may mimic a mastoid segment FNS, when it is contiguous with the primary tumor or seen as a skip lesion. History of known parotid gland malignancy should suggest the diagnosis (4, 8, 12, 13).

Intraparotid FNS can mimic a pleomorphic adenoma clinically, as well as on imaging (Fig. 14). Extension to the stylomastoid foramen and the tumor location along the posterolateral aspect of the retromandibular vein favor the diagnosis of an FNS (Fig. 15). However, these findings are not diagnostic for the FNS since pleomorphic adenomas, albeit rarely, may show extension to the stylomastoid foramen. Presence of a target sign on T2-weighted images, if seen, excludes the possibility of a pleomorphic adenoma.

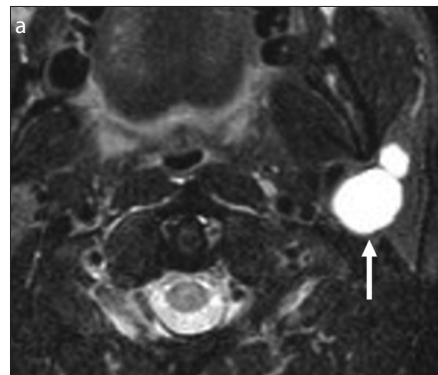
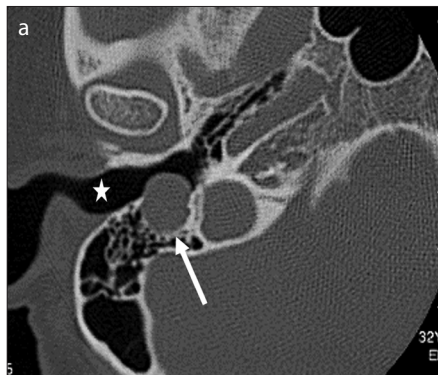


Figure 12. a, b. Axial (a) and coronal (b) HRCT images of the right temporal bone through posterior part of the mastoid show an FNS of the mastoid segment (a and b, *white arrow*) which is causing smooth erosion of the bony wall and protruding in the external auditory canal (a and b, *star*). Normal stylomastoid foramen (b, *black arrowhead*), middle ear cavity (b, *white arrowhead*), and lateral semicircular canal (b, *black arrow*) are seen.

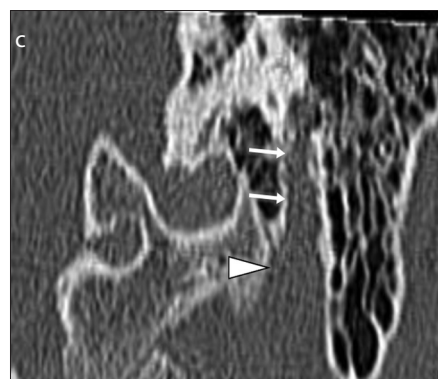
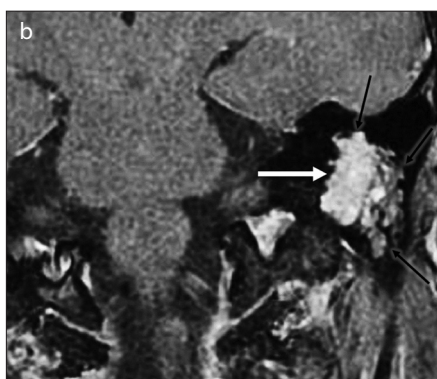
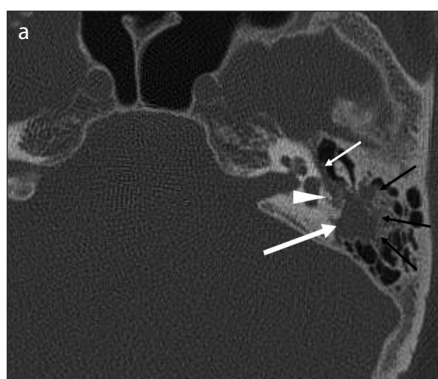


Figure 13. a, b. Axial HRCT (a) and postcontrast coronal T1-weighted image (b) of the left temporal show FNS of the mastoid segment (a and b, *thick white arrow*), which breaks through adjacent mastoid air cells and shows irregular margins (a and b, *thin black arrows*), and thus appears aggressive. Tumor extends to the posterior genu (a, *white arrowhead*) and the tympanic segment is normal (a, *thin white arrow*). Differential diagnosis includes aggressive lesions like metastasis or sarcoma.



Figure 14. Postcontrast axial CT scan shows an intraparotid FNS on left side (*white arrow*). Note its relation to the retromandibular vein (*black arrowhead*). The stylomastoid foramen shows normal fat density, which excludes extension of mass (*black arrow*). FNS in this location cannot be differentiated from a pleomorphic adenoma on imaging alone.

Parotid malignancies often have infiltrating margins and heterogeneous appearance on T2-weighted images. Nevertheless, perineural spread of parotid malignancies

should be included in the differential diagnosis of an intraparotid FNS showing extension along the stylomastoid foramen (3, 4, 14).

Treatment options

Treatment options for FNSs include surgical resection with nerve preservation, complete resection with nerve grafting, and decompression. The use of gamma knife radiosurgery is a relatively new and promising treatment option in cases of new or residual FNSs (15, 16).

Conclusion

Evaluation of the FNS requires a combined approach of correlating accurate clinical information with HRCT and MRI findings. Awareness of the imaging anatomy of the FN and the characteristic CT and MRI appearances of FNS involving different FN segments is crucial to arrive at the cor-

Figure 15. a–c. Axial (a) and coronal (b) T2-weighted fat-saturated image through the left parotid gland shows an intraparotid FNS (a, *arrow*). This mass shows extension to the stylomastoid foramen (b and c, *arrowhead*) and along the mastoid segment of the FN (b and c, *arrows*). Coronal HRCT image (c) through mastoid shows smooth expansion of the stylomastoid foramen and the mastoid segment of the FN.

rect diagnosis. Finally, the possible imaging differentials at various locations must be borne in mind so as to avoid potential diagnostic pitfalls.

Acknowledgements

The schematic representation of FNS in context of FN segment(s) in Fig. 5 was conceived and sketched by Dr. Bela Purohit.

Conflict of interest disclosure

The authors declared no conflicts of interest.

References

1. Fenton JE, Morrin MM, Smail M, Sterkers O, Sterkers JM. Bilateral facial nerve schwannomas. *Eur Arch Otorhinolaryngol* 1999; 256:133–135. [\[CrossRef\]](#)
2. Harnsberger HR, Glastonbury CM, Michel MA, Koch BL. *Diagnostic imaging: Head and neck*. 2nd ed. Altona: Amirsys, 2011; 6:14–17.
3. Shimizu K, Iwai H, Ikeda K, Sakaida N, Sawada S. Intraparotid facial nerve schwannoma: a report of five cases and an analysis of MR imaging results. *AJNR Am J Neuroradiol* 2005; 26:1328–1330.
4. Wiggins RH 3rd, Harnsberger HR, Salzman KL, Shelton C, Kertesz TR, Glastonbury CM. The many faces of facial nerve schwannoma. *AJNR Am J Neuroradiol* 2006; 27:694–699.
5. McMonagle B, Al-Sanosi A, Croxson G, Fagan P. Facial schwannoma: results of a large case series and review. *J Laryngol Otol* 2008; 122: 1139–1150. [\[CrossRef\]](#)
6. Hasan NU, Kazi T. Malignant schwannoma of facial nerve. *J Pediatr Surg* 1986; 21:926–928. [\[CrossRef\]](#)
7. Sunderland S. Some anatomical and pathophysiological data relevant to facial nerve injury and repair. In: Fisch U, ed. *Facial nerve surgery*. Amstevleen: Kugler, 1977; 47–67.
8. Kertesz TR, Shelton C, Wiggins RH, Salzman KL, Glastonbury CM, Harnsberger R. Intratemporal facial nerve neuroma: anatomical location and radiological features. *Laryngoscope* 2001; 111:1250–1256. [\[CrossRef\]](#)
9. Guinto EJ, Himadi GM. Tomographic anatomy of the ear. *Radiol Clin North Am* 1974; 12: 405–417.
10. Gupta S, Mends F, Hagiwara M, Fatterpekar G, Roehm PC. Imaging the facial nerve: a contemporary review. *Radiol Res Pract* 2013; 248039: 1–14. [\[CrossRef\]](#)
11. Salzman KL, Davidson HC, Harnsberger HR, et al. Dumbbell schwannomas of the internal auditory canal. *AJNR Am J Neuroradiol* 2001; 22:1368–1376.
12. Chung SY, Kim DI, Lee BH, Yoon PH, Pyoung J, Chung TS. Facial nerve schwannomas: CT and MR findings. *Yonsei Med J* 1998; 39:148–153. [\[CrossRef\]](#)
13. Phillips CD, Hashisaki G, Vellion F. Anatomy and development of the facial nerve. In: Swartz JD, ed. *Imaging of temporal bone*. 4th ed. New York: Theime, 2009; 444–479.
14. Nader ME, Bell D, Sturgis EM, Ginsberg LE, Gidley PW. Facial nerve paralysis due to a pleomorphic adenoma with the imaging characteristics of a facial nerve schwannoma. *J Neurol Surg Rep* 2014; 75: 84–88. [\[CrossRef\]](#)
15. McMonagle B, Al-Sanosi A, Croxson G, Fagan P. Facial schwannoma: results of a large case series and review. *J Laryngol Otol* 2008; 122:1139–1150. [\[CrossRef\]](#)
16. Madhok R, Kondziolka D, Flickinger JC, Lunsford LD. Gamma knife radiosurgery for facial schwannomas. *Neurosurgery* 2009; 64:1102–1105. [\[CrossRef\]](#)